

---

## Impact of an intrusion by the Northern Current on the biogeochemistry in the eastern Gulf of Lion, NW Mediterranean

Ross Oliver N.<sup>1,\*</sup>, Fraysse Marion<sup>1,2</sup>, Pinazo Christel<sup>1</sup>, Pairaud Ivane<sup>2</sup>

<sup>1</sup> Aix-Marseille University, CNRS, University of Toulon, IRD, MIO UM 110, 13288, Marseille, France

<sup>2</sup> Institut Français de Recherche pour l'Exploitation de la Mer, Laboratoire Environnement Ressources Provence Azur Corse, F-83507 La Seyne sur Mer, France

\* Corresponding author : Oliver N. Ross, email address : [oliver.ross@univ-amu.fr](mailto:oliver.ross@univ-amu.fr)

---

### Abstract :

We present the results from the RHOMA2011-LEG2 campaign that took place in the eastern Gulf of Lion from 7 to 17 Oct 2011 and combine them with remote sensing observations and results from a 3D coupled hydrodynamic-biogeochemical model to study an intrusion event of the Northern Current (NC) onto the continental shelf in the Gulf of Lion (NW Mediterranean). Our analysis shows that during the intrusion, the previously upwelled nutrient-rich water present on the shelf is replaced by warmer and mostly oligotrophic NC water within a matter of 2–3 days. This has a marked impact on the local biogeochemistry in the Gulf with pre-intrusion Chl-a concentrations in the surface layer of over 0.5 mg m<sup>-3</sup> dropping to near the detection limit within less than 72 h. The intrusion event leads to a dramatic albeit short-lived regime shift in the limiting nutrient for primary production: prior to the intrusion most of production on the shelf is nitrogen limited while the intrusion induces a shift to phosphorous limitation. The relatively high frequency of occurrence of these intrusions in combination with their impact on the local ecosystem make them primary targets for future study.

### Highlights

► An Intrusion event of the Northern Current was observed and modelled in the Gulf of Lion. ► Intrusions can completely flush the eastern Gulf of Lion within 2–3 days. ► Intrusions can produce dramatic short-lived regime shifts in the local biogeochemistry.

**Keywords :** Northern Current, Gulf of Lion, Intrusion, Continental shelf, Biogeochemical modelling, Regime shift

48 The continental shelf of the Gulf of Lion (GoL) in the NW Mediterranean Sea offers a  
49 typical system for studying river/shelf/open sea interactions. Due to the Rhone River and  
50 frequent upwelling events, the GoL is one of the most productive areas in a mostly  
51 oligotrophic Mediterranean Sea [de Madron *et al.*, 2011].

52 The circulation in the GoL is forced mainly by wind, freshwater run-off and seasonal  
53 heating–cooling [Millot, 1990]. The dominant circulation feature is the Northern Current  
54 (NC, Figure 1a), a slope current that passes along the continental slope off the GoL, where it  
55 bounds and controls shelf circulation, effectively separating the typically nutrient rich shelf  
56 from the oligotrophic open Mediterranean. It originates from the confluence of the Eastern  
57 and Western Corsican Currents and flows from the Ligurian to the Balearic Sea forming part  
58 of the general cyclonic circulation in the Western Mediterranean.

59 The NC exhibits a seasonally variable flux (maximal in winter) between 1-2Sv which  
60 is comparable to the fluxes through the Strait of Gibraltar [Alberola *et al.*, 1995]. The NC is  
61 wider and shallower in summer (50km and 250m respectively) when it flows further off-  
62 shore. In winter, it moves in-shore where it narrows and deepens (ca. 30km and 450m)  
63 reaching maximal velocities of over  $50\text{cm s}^{-1}$  [Andre *et al.*, 2009]. Particularly in winter, the

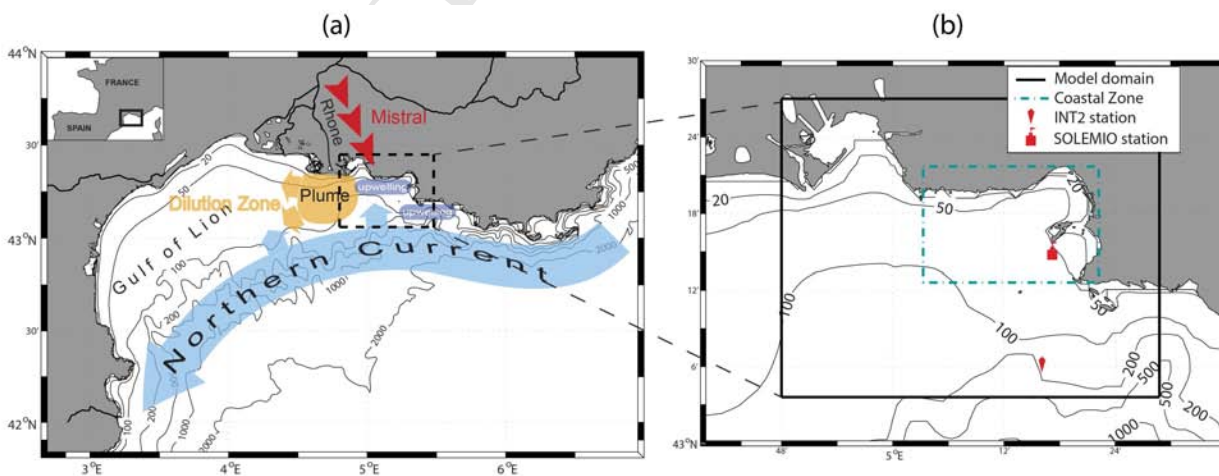


Figure 1: (a) Map of the Gulf of Lion showing the location of the study area at the eastern entrance (dashed box) and the dominant hydrodynamic and meteorological features, including the Northern Current and its northward intrusions onto the shelf. (b) Zoom of the study area, showing the location of the coastal zone budget box and the INT2 and SOLEMIO observational stations.

64 NC also becomes baroclinically unstable and produces important mesoscale meanders which  
65 can penetrate onto the GoL shelf [Millot, 1999; Petrenko, 2003; Rubio *et al.*, 2009].

66 These intrusions of the NC can occur at various places along the shelf. Most  
67 frequently, they tend to occur at the eastern entrance to the Gulf [Petrenko *et al.*, 2005] and at  
68 the center [Estournel *et al.*, 2003], with more rare occurrences at the south-western side  
69 [Petrenko *et al.*, 2008]. Using data from 12 coastal cruises, Gatti *et al.* [*Intrusions of the*  
70 *Mediterranean Northern Current on the eastern side of the Gulf of Lion's continental shelf:*  
71 *characterization and generating processes, submitted to Journal of Geophysical Research*  
72 *2015*] found that intrusions can occur during any season of the year and that the intrusion flux  
73 can amount to 0.37 SV or 30% of the flux of the NC itself. They also carried out numerical  
74 realistic simulations which suggest that intrusions can occur as often as three to four times  
75 per month with durations of a few days to two weeks. By combining *in situ* observations and  
76 high-resolution modelling, Barrier *et al.* [2015] observed a total of 12 intrusion events during  
77 their 12 month study period, although they state that the amount of observational data in  
78 particular is not sufficient to capture all intrusion events and they only counted very large  
79 intrusions in their analysis.

80 Three kinds of wind events are likely to generate intrusions: cessations of strong  
81 Mistral events [Millot and Wald, 1980], episodes of inhomogeneous Mistral, or periods of  
82 easterly winds [Petrenko, 2003; Petrenko *et al.*, 2013]. NC intrusions onto the shelf have also  
83 been linked to the strength of density stratification and the pycnocline depth with the NC  
84 splitting into a main and a northern branch, the latter creating an intrusion if the stratification  
85 is strong and shallow [Echevin *et al.*, 2003; Petrenko *et al.*, 2005]. However, other studies  
86 showed that intrusions at the eastern entrance to the GoL could occur independently of  
87 stratification [Petrenko, 2003]. These seemingly contradicting results suggest that the real  
88 causes of intrusions are still unclear [Petrenko *et al.*, 2005] although the shift in the local  
89 wind regime may play a crucial role [Pairaud *et al.*, 2011; Petrenko *et al.*, 2008]. Barrier *et*

90 *al.* [2015] suggested that intrusions on the eastern part of the gulf are mainly forced by

91 easterly or north-westerly wind events and they found them to be most frequent in the autumn  
92 and winter months.

93 While the Northern Current (NC) and its intrusions onto the continental shelf in the  
94 Gulf of Lion have been widely studied from a hydrodynamical point of view [*Alberola and*  
95 *Millot, 2003; Petrenko, 2003*], including intrusions in the eastern GoL [*Pairaud et al., 2011;*  
96 *Petrenko et al., 2008*], little is known about the impact of these intrusions on the  
97 biogeochemistry. The biogeochemical functioning of the eastern GoL is complex and largely  
98 driven by the interplay of Rhone River run-off, hydrodynamics, and air-sea interactions. The  
99 Rhone River is the most significant source of freshwater and nutrients to the Mediterranean  
100 Basin with a flux of 2–20 Mt yr<sup>-1</sup> [*Sempere et al., 2000*]. This has a great impact on the  
101 biogeochemical functioning of the GoL and directly affects primary production: about 50%  
102 of the annual primary production in the GoL can be attributed to terrigenous inputs [*Coste,*  
103 *1974; Morel et al., 1990*]. Typically the Rhone River Plume extends westward but eastward  
104 intrusions of plume water into the Bay of Marseille (inside our study area) have also been  
105 observed [*Fraysse et al., 2014; Gatti et al., 2006*]. The variability in the Rhone River run-off  
106 also has a measurable impact on the fisheries industry. In a study covering a nearly 30-year  
107 period from 1973-2000, a correlation was found between the interannual variability of the  
108 Rhone River run-off and the landings of Common Sole (*Solea solea*) 5 years later,  
109 particularly in the eastern GoL port of Martigues where about 50% of landings for the GoL  
110 are recorded (M. Harmelin, pers. comm.).

111 In addition, two dominant winds act as important forcing components: (i) north-  
112 westerlies (Mistral in Figure 1), which favour upwelling [*Millot, 1990*], and (ii) south-  
113 easterly winds, which favour downwelling [*Fraysse et al., 2014; Pairaud et al., 2011*].  
114 During an upwelling event, cold, nutrient-rich waters are brought up to the euphotic zone [*El*  
115 *Sayed et al., 1994*], which can lead to an increase in primary production.

116 Here we explore the impact of intrusions by the Northern Current onto the eastern  
117 GoL shelf area, just after an upwelling event, focussing primarily on the effect on the local  
118 biogeochemistry. This is achieved through combining results from a 3D coupled  
119 hydrodynamical-biogeochemical model of the region with *in situ* (nutrients, chl, current  
120 velocities) and remote sensing observations (SST, Ocean colour). The analysis shows that NC  
121 intrusions can have a significant impact on the shelf biogeochemistry and bring about a  
122 dramatic regime shift in the local ecosystem within a rather short period of time that lasts for  
123 the duration of the intrusion event.

## 124 **2. Materials and Methods**

### 125 **2.1. Field sampling and remote sensing data**

126 All observational *in situ* data collected between 7 to 17 October 2011 stems from the  
127 RHOMA2011-LEG2 campaign that took place in the eastern Gulf of Lion (Figure 1). The *in*  
128 *situ* data was collected aboard RV Tethys II using an SBE19PlusV2 CTD that was also  
129 equipped with an optical backscatter sensor (Campbell Scientific OBS3+) and a fluorimeter  
130 (WetLabs WetStar). In addition, discrete water samples were collected at various depths for  
131 nutrient analysis and for calibration of the fluorescence data [see Materials and Methods in  
132 *Frayse et al.*, 2013 for details on *in situ* data collection and processing]. The current  
133 velocities and directions were obtained from the 150 kHz hull-mounted Acoustic Doppler  
134 Current Profiler (ADCP) of the RV Tethys II. Currents were recorded along the vessel's track  
135 over the course of several hours each day. ADCP data for 18 October 2011 stems from the  
136 SPECIMED campaign that took place every month between 2010 and 2014, and was  
137 collected with a 300 kHz ADCP mounted on a towed fish that was suspended from the  
138 vessel's side at a depth of between 1-2m.

139 These *in situ* data were combined with remote sensing observations of sea surface  
140 temperature (SST) and of ocean colour. The SST information was taken from the Level 3

141 SST multisensory products available from the MyOcean database (dataset: SST-  
142 EUR\_L3S\_NRT\_OBSERVATIONS\_010\_009\_a). These data come at a horizontal resolution  
143 of  $0.02^\circ$  and are typically collected at night to reduce potential errors due to the skin effect. In  
144 an attempt to further control the skin effect we used mooring data from the “Le Planier”  
145 mooring at ( $43.21^\circ\text{N}$ ,  $5.23^\circ\text{E}$ ) to calibrate the satellite SST. The average offset between the  
146 mooring and the satellite derived SST during our period of study was  $+1^\circ\text{C}$  which suggested  
147 that some skin effect remained which we subtracted from the satellite data. Each SST pixel  
148 represents the daily mean collected from various sensors. One single snapshot thus represents  
149 a collage of values collected over a range of up to 12h.

150 The ocean colour data originated from the MODIS platform and were processed using  
151 the OC5 algorithm [Gohin *et al.*, 2005] to obtain chlorophyll-*a* concentrations (Chl-*a*). The  
152 horizontal resolution is about 1.1km and due to the OC5 algorithm they have a lower  
153 detection threshold for Chl-*a* of  $0.1 \text{ mg m}^{-3}$ .

## 154 2.2. The model

155 The hydrodynamic model MARS3D [Lazure and Dumas, 2008] was used in the  
156 RHOMA configuration [Peraud *et al.*, 2011] coupled to the ECO3M biogeochemical  
157 platform [Baklouti *et al.*, 2006a; Baklouti *et al.*, 2006b] in the MASSILIA-P configuration  
158 [Frayse *et al.*, 2014; Fraysse *et al.*, 2013]. The model structure is primarily based on the  
159 pelagic plankton ecosystem model that was published previously [Faure *et al.*, 2010a; Faure  
160 *et al.*, 2010b; Pinazo *et al.*, 1996]. It contains 5 compartments (phytoplankton, heterotrophic  
161 bacteria, dissolved and particulate organic matter and dissolved inorganic matter) and allows  
162 for a variable intracellular content of carbon, nitrogen and phosphorous in the phytoplankton  
163 and bacteria groups. The physical-biogeochemical coupled model was applied to the eastern  
164 GoL at a horizontal resolution of 400 m using 30 vertical sigma levels. The model run  
165 covered the years 2007-2011 and is in its setup (spin-up, boundary conditions, parameter

166 values, etc.) identical to the one described in detail in *Fraysse et al.* [2013, Materials and  
167 Methods]. The values for the biogeochemical parameters at the open boundary were chosen  
168 based on a sensitivity analysis with difference OBCs to deliver results that were in best  
169 quantitative agreement with observations at the fixed stations within the model domain  
170 (where nutrient samples were taken) and also with observations from remote sensing chl data.

171 Two different approaches were used for comparing the model results to observations  
172 of velocities and temperature. For the quantitative comparison of the model with ADCP  
173 velocities, we used a model output every 10 minutes such that the error in synopticity is no  
174 larger than +/- 5 minutes. When comparing the model SST with the satellite image, we used  
175 the collection time of each pixel in an image to obtain the mean time and chose the closest  
176 model time step for the comparison.

177 The same applies for the comparison of the MODIS image with the model surface  
178 concentrations of Chl-*a*. In order to provide a fair visual comparison between the model data  
179 and satellite images, all model values of Chl-*a* less than the OC5 algorithm's detection limit  
180 have been set to 0.1 mg m<sup>-3</sup>.

181 For all satellite/model comparisons, the satellite data was interpolated onto a  
182 horizontal 400×400m grid to match the model resolution. The mass budgets were calculated,  
183 based on equations 3 and 4 from [*Fraysse et al.*, 2014].

### 184 **3. Results**

185 The wind pattern during the study period is characterized by a 1-week period of  
186 strong Mistral winds that lasted from about 7-13 October 2011, followed by two days of  
187 strong easterlies (Figure 2). The Mistral caused a persistent upwelling event along the coast,  
188 the last stages of which are still visible on the SST snapshot from 13 October (Figure 3a, b)  
189 where the upwelled water can be identified from the relatively cold water all along the coast.

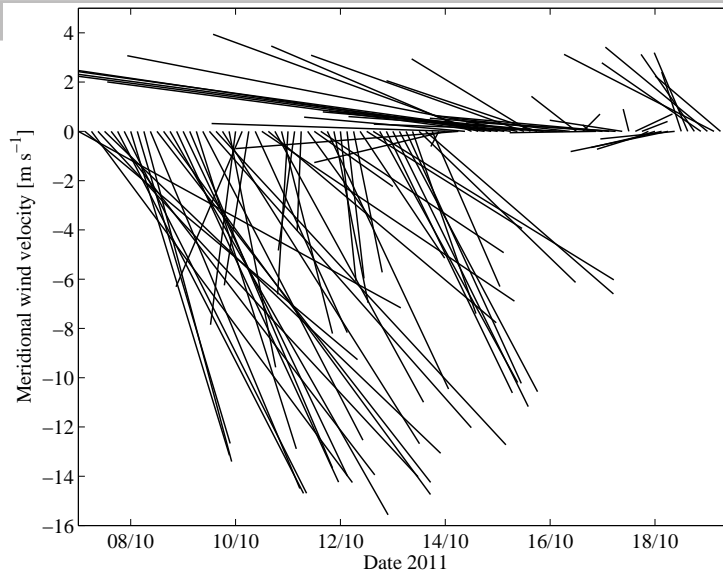


Figure 2: MM5 (5th generation PSU/NCAR mesoscale) model wind vectors near the SOLEMIO station (at 43.25°N, 5.27°E). Visible is the strong Mistral event from the 7<sup>th</sup> till the 13<sup>th</sup>, followed by a short period of strong easterlies and relative calm from the 17<sup>th</sup> onward.

190 This upwelling event brought higher concentrations of nutrients to the surface layer and  
 191 created a short-lived bloom (see Fraysse [2014] for details). In comparison to the SST  
 192 estimates from satellites, the model captures both the magnitude and location of the  
 193 upwelling event quite well.

194 At the same time, the Northern Current (NC) is present with maximal velocities of  
 195 over  $0.5 \text{ m s}^{-1}$  and it begins to intrude onto the continental shelf in the eastern Gulf of Lion  
 196 (Figure 3). The intrusion starts on 13 October 2011 and is characterized by the emergence of  
 197 a strong shoreward component of the velocity vectors which is visible in both the model  
 198 simulations and *in situ* observations (Figure 3a).

199 On 16 October 2011, both the velocity and temperature images show that the cooler  
 200 onshore water that was present only three days earlier has now been replaced with warmer  
 201 water from the NC (Figure 3c-d). The intrusions of the warmer NC water led to a rise in the  
 202 surface water temperature on the shelf of up to  $4^{\circ}\text{C}$ . The onshore velocity vectors reach  
 203 values of over  $0.6 \text{ m s}^{-1}$  and the location of the velocity maximum has moved slightly  
 204 westward. We begin to see the development of an anticyclonic eddy, the so-called Marseille  
 205 Eddy [Schaeffer *et al.*, 2011]. Vertical velocity profiles confirm that the intrusion is not only  
 206 limited to the surface layer but extends to depths of at least 70m as we have significant on-



207 shore velocity components at depths beyond 65m (Figure 3e). By comparing the observed  
 208 and modelled velocities, we find that the model tends to generally overestimate *in situ*  
 209 velocities on the shelf (Figure 3f), while underestimating the velocities further offshore (the  
 210 mean weighted difference over all depths and locations is  $0.014 \text{ m s}^{-1}$  with an RMSE of  $0.1 \text{ m}$

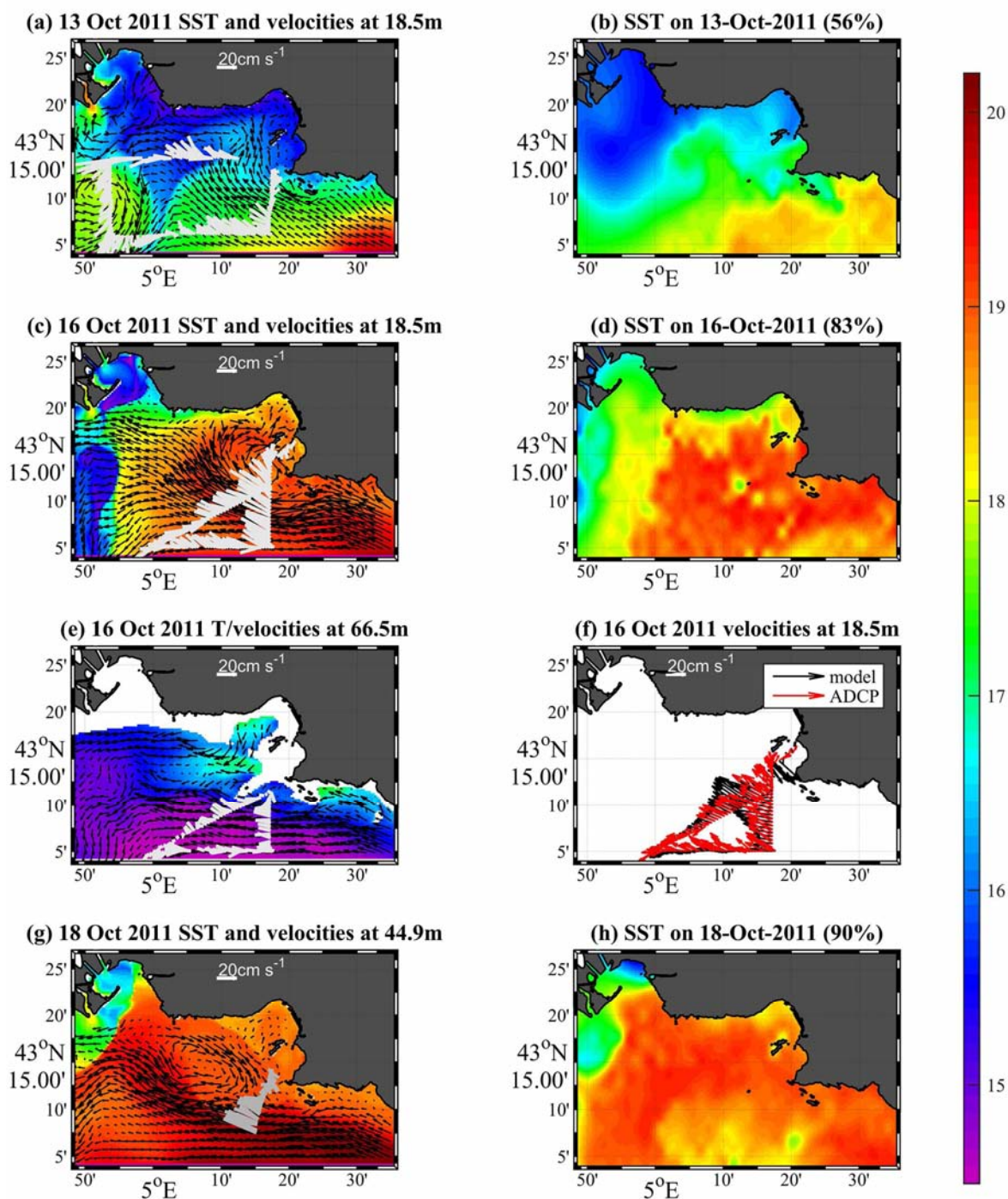


Figure 3: (a) Model velocities (black arrows) with measured ADCP velocities (light grey bars) at a depth of 18.5m on 13 Oct 2011 superimposed on modelled SST. (b) Remotely sensed SST for 13 Oct 2011 (the percentage in brackets gives the satellite coverage for that day). Corresponding plots for (c-d) 16 Oct 2011 and (g-h) 18 Oct 2011. (e) as in (c) but with both the temperature and velocities at 66.5m. (f) Comparing modelled with measured velocities along the ship track at 18.5m depth. The color scale is in  $^{\circ}\text{C}$ .

211  $s^{-1}$ ). A tendency for the model to underestimate the currents associated with the NC intrusions  
 212 in the south-eastern part of the model domain was also observed during the event of October  
 213 2007 described by *Pairaud et al.* [2011]. Nevertheless, the predominant north-westward  
 214 current direction is generally well reproduced by the model, except at the southern boundary.

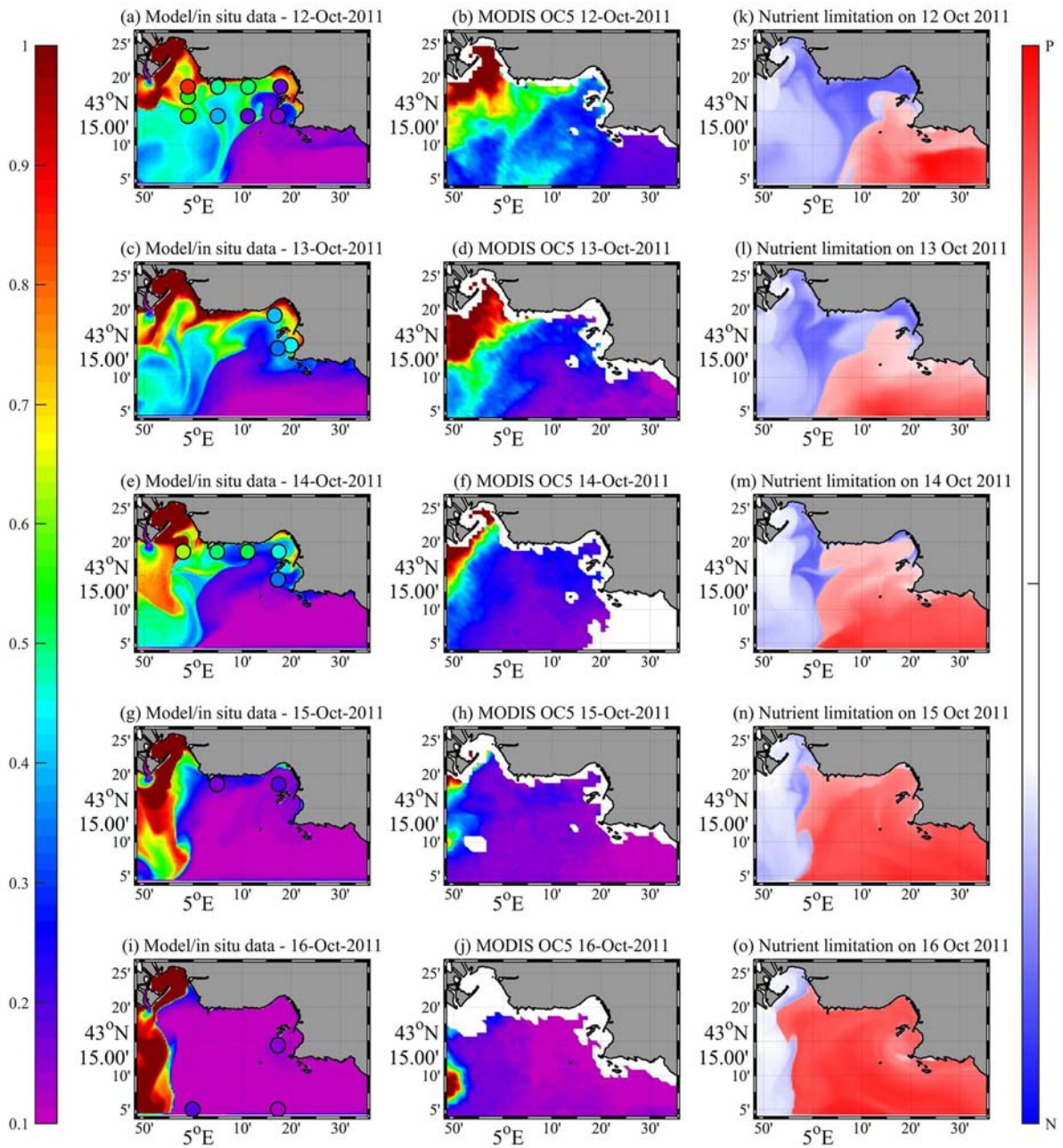


Figure 4: (a) In situ observations of surface Chl-a (filled circles, various times of the day) superimposed on the modelled surface Chl-a concentrations (at 12:00h) for 12 Oct 2011. (b) MODIS image for the same date. Corresponding images for (c-d) 13 Oct 2011, (e-f) 14 Oct 2011, (g-h) 15 Oct 2011 and (i-j) 16 Oct 2011. The color scale on the left is valid for panels (a) through (j) and is in  $mg\ m^{-3}$ . Panels (k) to (o) have their own color scale on the right and show the modelled nutrient limitation in the surface layer for the same dates as before. Red colors signify that photosynthesis is phosphorous limited, blue colors indicate limitation by nitrogen and white colors suggest little or no limitation. The color intensity corresponds to the strength of the limitation.

215 By 18 October 2011, the westward progression of the velocity maximum had

216 continued and the Marseille Eddy was fully developed, extending to depths of about 50m  
217 (Figure 3g). The SST on the shelf is now fairly homogeneous and close to 20°C.

218 This particular intrusion event of the NC had been directly preceded by an episode of  
219 strong north-westerly Mistral winds which had induced an upwelling near the coast which in  
220 turn led to an increase in local surface Chl-*a* concentrations to values of between 0.5 to 0.6  
221 mg m<sup>-3</sup> in the upwelling zone (Figure 4a, b). On 13 October 2011, this upwelling event was  
222 still in progress (cf. temperature distribution in Figure 3a-b) and both model simulations and  
223 satellite images show high Chl-*a* concentrations near the coast (Figure 4c, d). Due to the  
224 inherent difficulties for the remote sensing algorithms near the coast [Antoine *et al.*, 2008],  
225 we have no satellite estimates in the most shallow areas but given its error margin of about  
226 30% [Volpe *et al.*, 2012], the remote sensing data is in good agreement with the *in situ*  
227 observations as well as the model hindcasts. As the intrusion event progresses in time and  
228 space, surface Chl-*a* concentrations gradually drop to values of about 0.1 mg m<sup>-3</sup> throughout  
229 the eastern Gulf (Figure 4e-j). This is also visible in the satellite images where the Chl-*a*  
230 concentrations drop to near the OC5 algorithm's detection limit of 0.1 mg m<sup>-3</sup> on 16 October  
231 2011 (Figure 4j).

232 In the model, phytoplankton primary production is controlled by the most limiting  
233 internal nutrient ratio, i.e., either the intracellular N:C or P:C ratio (cf. Eq. 4 in Fraysse *et al.*  
234 [2013]). Commensurate with simulation results of an upwelling event that took place in 2008  
235 (cf. Fig 9b in Fraysse *et al.* [2013]), we found that the rates of phytoplankton photosynthesis  
236 tend to be nitrogen rather than phosphorous limited in the upwelling zone (Figure 4k). In fact,  
237 the model domain is clearly divided into an N limited coastal (upwelling) area and a P limited  
238 region which corresponds to the Northern Current. The Rhone River plume to the west is  
239 nutrient replete and only light limited which can be seen from the almost white colour in that  
240 area which indicates that the cellular nutrient-to-carbon ration is high, both for N:C and P:C.

Table 1: In situ surface values in units of  $\text{mg m}^{-3}$  for the principal nutrients collected at SOLEMIO station over the course of the upwelling (12/13 October) and the intrusion (16/17 October).

	12 Oct 2011	13 Oct 2011	16 Oct 2011	17 Oct 2011
NO <sub>3</sub>	0.12	0.28	0.06	0.13
NH <sub>4</sub>	0.93	0.80	0.32	0.27
PO <sub>4</sub>	0.11	0.12	0.06	0.02

241 As the NC intrusion progresses, the model suggests an increasing phosphorous limitation on  
 242 the shelf (Figure 4l through o). On 18 October (not shown) photosynthesis rates over the  
 243 entire domain (apart from the Rhone River plume) are P limited (commensurate with the  
 244 extent of the  $\sim 20^\circ\text{C}$  isothermal on the SST image in Figure 3h). The fact that the intrusion of  
 245 warmer NC water also led to the intrusion of oligotrophic water onto the shelf was confirmed  
 246 by the analyses of *in situ* water samples. While pre-intrusion (12 Oct 2011) phosphate levels  
 247 in the surface layer could locally reach values of the order of  $0.1 \mu\text{M}$  (Table 1), the  
 248 concentrations dropped to very low values once the intrusion was in full swing (16/17 Oct  
 249 2011) (Table 1 and 2). For nitrate and ammonium, the surface layer was also completely  
 250 depleted by 16 October 2011 although there was some ammonium present at depth which  
 251 may be linked to the sizable Chl-*a* concentration there (Table 2).

Table 2: In situ data collected at station INT2 ( $43^\circ 5' \text{N}$ ,  $5^\circ 17' \text{E}$ ) on 16 October 2011.

Depth (m)	Chl- <i>a</i> ( $\text{mg m}^{-3}$ )	NH <sub>4</sub> ( $\mu\text{M}$ )	NO <sub>3</sub> ( $\mu\text{M}$ )	PO <sub>4</sub> ( $\mu\text{M}$ )
0	0.11	no data	0.02	0.06
15	0.13	0.28	0.00	0.02
40	0.22	0.22	0.00	0.01
60	0.26	0.20	0.00	0.01
80	0.32	0.42	0.05	0.02
100	0.14	no data	0.04	0.12

253 on the shelf (Figure 5). By 16 October the intrusion has replaced the cooler shelf water,  
 254 which had been upwelled prior to 13 October, with warm water from the NC (Figure 5a, b).  
 255 At the same time, the deep chlorophyll maxim that was present on 13 October has also been

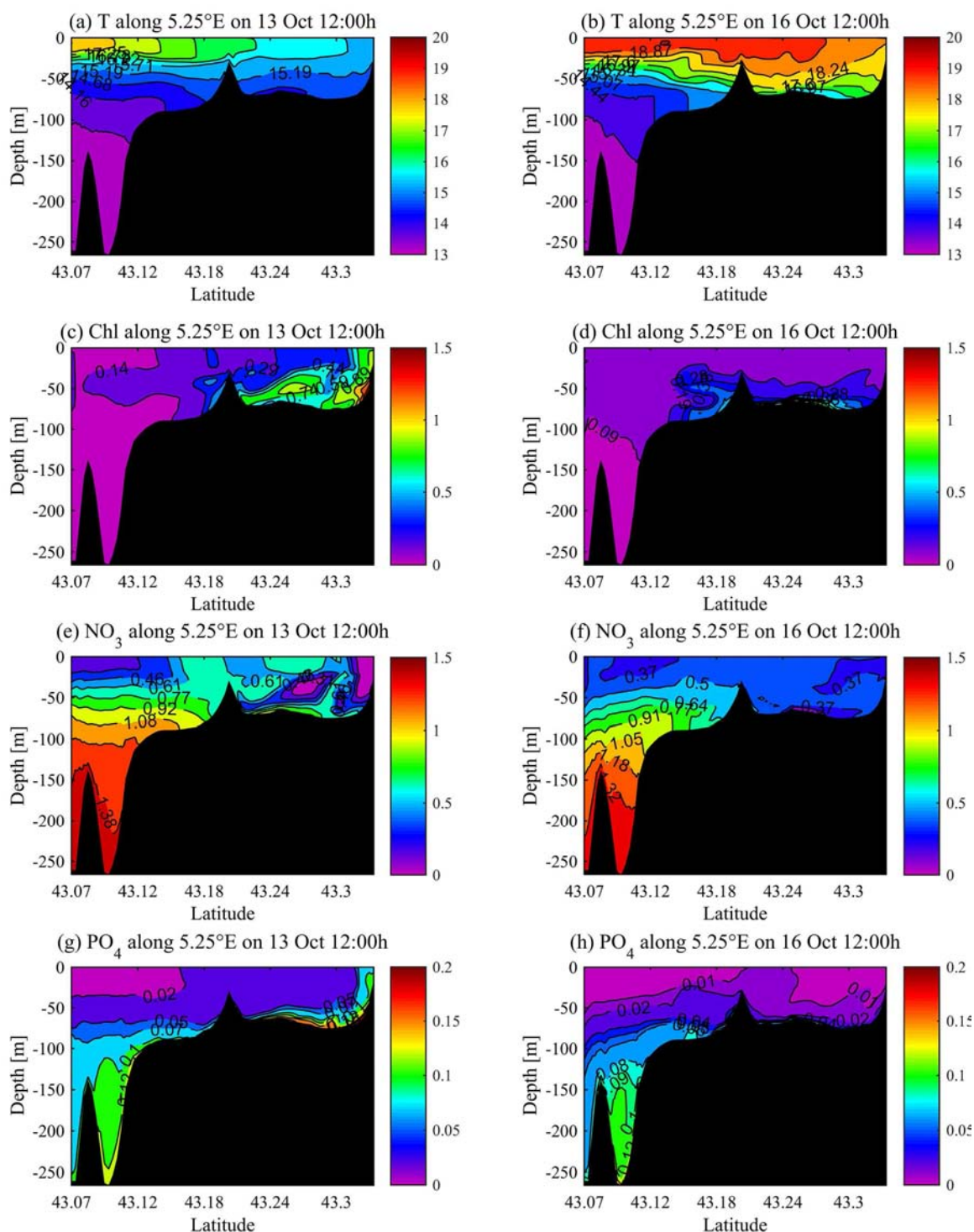


Figure 5: Vertical sections along 5° 15' E on 13 Oct (post-upwelling/pre-intrusion) and 16 Oct (mid intrusion) showing (a,b) water temperature in °C; (c,d) chl-a concentration in  $\text{mg m}^{-3}$ ; (e,f)  $\text{NO}_3$  concentration in  $\text{mmol L}^{-1}$ ; and (g,h)  $\text{PO}_4$  concentration in  $\text{mmol L}^{-1}$ .

256 removed and values are below  $0.1 \text{ mg m}^{-3}$  down to about 50m (Figure 5c,d). On 13 October,  
 257  $\text{NO}_3$  is very low in the areas affected by the upwelling along the coast (Figure 5e) while  $\text{PO}_4$   
 258 is increased at the same time (Figure 5g). Three days later,  $\text{NO}_3$  concentrations have  
 259 increased near the coast (to about  $0.34 \text{ mmol L}^{-1}$ , Figure 5f) while  $\text{PO}_4$  concentration have  
 260 dropped to less than  $0.01 \text{ mmol L}^{-1}$  in the surface layer (Figure 5h).

261 In order to further characterize the changes in the biogeochemistry due to the NC  
 262 intrusion event, we calculated the changes in the mass budgets [see equations 3 and 4 in  
 263 *Frayse et al.*, 2014] for some of the model variables. For this purpose we focus on a coastal  
 264 sub-zone (Figure 1b), which contains most of the larger upwelling areas but excludes the  
 265 Rhone delta which lies a few kilometres to the west and also the normal path of the NC  
 266 further offshore. The results (Figure 6) show an increase in the biological production of  
 267 carbon associated with increases due to advective processes of the two main nutrients, N and  
 268 P, during the upwelling period from 7 till the 13 October 2011. Most of the new production  
 269 ( $B^{\text{BIO}}$  in Figure 6) is exported almost immediately (via  $B^{\text{OB}}$ ), which leaves the total budget  
 270 ( $B^{\text{TOT}}$ ) unchanged, or even slightly negative due to the losses through the open boundaries.

271 With the onset of the intrusion of the Northern Current, around 13 October, we  
 272 observed a significant change in the mass budgets. The new production of carbon levels off,  
 273 and the losses through the open boundaries reach their maximum as the previously produced  
 274 carbon is simply swept out of the box by the inflow of oligotrophic water from the Northern

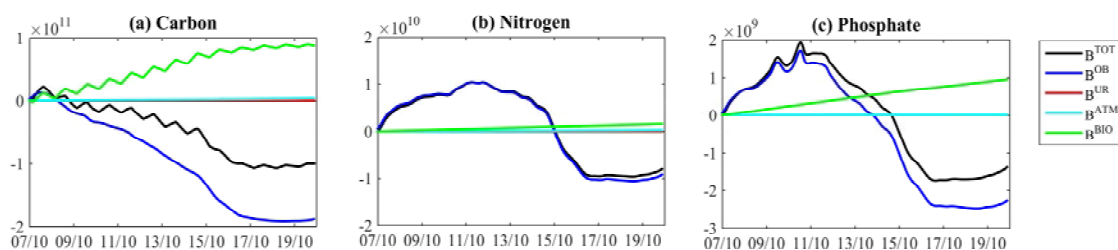


Figure 6: Mass budgets for (a) total carbon, (b) total nitrogen and (c) total phosphorous for the coastal zone box shown in **Error! Reference source not found.b** and the period covering the upwelling (7-13 October) and subsequent intrusion of the Northern Current. The curves show **cumulative** changes in total mass (depth integrated) relative to 7 October 2011; hence absolute values are not representative of the instantaneous state of the system but show the accumulated change relative to day 0, while the gradients give an indication of instantaneous changes (fluxes). The curves represent changes in the total mass budget (TOT) due to losses/gains through the open boundaries (OB), input by urban rivers (UR) and atmospheric deposition (ATM), as well as changes due to biological processes (BIO).

275 Current. This can be seen from the rather steep gradients between 14 and 16 of October. The  
276 same trends can be observed for the two main nutrients which exhibit a sharp decline in their  
277 standing stock.

#### 278 **4. Discussion**

279 We examined an intrusion event of the Northern Current onto the continental shelf in  
280 the eastern Gulf of Lion (NW Mediterranean). Such intrusions had been observed [*Petrenko*  
281 *et al.*, 2005; *Petrenko et al.*, 2013] but their impact on the local biogeochemistry had not been  
282 studied until now.

283 The intrusion event that took place between 13 to 18 October 2011 was preceded by  
284 several days of strong ( $> 15 \text{ m s}^{-1}$ ) north- to north-westerly winds (Mistral) which ceased on  
285 14 October with the wind direction turning to easterly (Figure 2). The sustained Mistral had  
286 led to upwelling events along the coast of the Bay of Marseille with the introduction of cooler  
287 phosphorous-rich water into the surface layer (Figure 3a, b) and associated increases in Chl-*a*  
288 used as a proxy for phytoplankton primary production (Figure 4a-d).

289 We could clearly identify the intrusion event based on the modelled and measured  
290 velocity fields which exhibited a clear and sustained on-shelf velocity component at the  
291 eastern entrance to the Gulf (Figure 3). Within a time frame of 2 to 3 days, the intrusion event  
292 led to a marked change in the temperature structure on the shelf, replacing the previously  
293 upwelled nutrient-rich cool water with warmer oligotrophic water from the Northern Current.  
294 The effect was so dramatic that within only 2-3 days the entire region had its surface  
295 temperature increased by about  $4^{\circ}\text{C}$  (Figure 3) and the average Chl-*a* concentration reduced  
296 by about  $0.3\text{-}0.4 \text{ mg m}^{-3}$  (Figure 4). In good agreement with previous studies [*Petrenko et al.*,  
297 2005; *Petrenko et al.*, 2013], we found that the intrusion had an impact over the entire water  
298 column with discernible on-shore velocity components and effects on ambient nutrient  
299 concentration being observed down to a depth of about 80m (cf. Figure 5).

301 the eastern GoL to be of the order of about 0.5 Sv [Petrenko *et al.*, 2005] and 0.37 Sv  
302 [Petrenko *et al.*, 2013] respectively. We calculated that for each day that such a flux persists,  
303 it would replace about 20-25% of the on-shelf water north of 43.1°N and east of 4.6°E.  
304 Considering the speed with which the temperature and Chl-*a* structure on the shelf changed  
305 (cf. Figure 3 and 5), we could hypothesize that the on-shelf fluxes during the October 2011  
306 intrusion may have been of the same order of magnitude or maybe even slightly higher,  
307 although neither SST nor Chl-*a* alone are sufficiently reliable indicators. Using the modelled  
308 zonal velocities, we calculated an average on-shelf (northward) flux of about 0.45 Sv across a  
309 line at 43.07°N between 15 and 18 October 2011 with short-term peak values reaching about  
310 0.65 Sv. However, considering that the model tends to slightly overestimate the velocities  
311 measured by the ADCP (cf. Figure 3f), these values may only be slightly too high.

312 It is difficult to generalize the effect that such an intrusion would have on the  
313 biogeochemistry because its impact strongly depends upon the state of the ecosystem at the  
314 time the intrusion occurs. During the already oligotrophic summer months, for instance,  
315 intrusions of oligotrophic NC water would have a much more subdued effect compared to an  
316 intrusion that was to occur during a bloom period. Blooms in the eastern GoL can be of a  
317 seasonal nature, or be caused by short-lived events such as Mistral-induced upwellings or  
318 Rhone River intrusions advecting nutrient-rich Rhone water from the west [Frayse *et al.*,  
319 2014]. For our particular study period in October 2011, the impact was significant as the  
320 region had been experiencing a sustained period of Mistral and associated upwelling  
321 immediately prior to the intrusion which led to the presence of relatively nutrient rich waters  
322 and an increase in local primary production. The intrusion that began on 13 October 2011 put  
323 a sudden stop to this mini-bloom. Chl-*a* concentrations of previously over 0.5 mg m<sup>-3</sup>  
324 dropped to values of less than 0.2 mg m<sup>-3</sup> throughout the eastern Gulf within a matter of 2 to  
325 3 days (Figure 3a through j). Also the nutrient concentrations decreased significantly and the



326 shelf water quickly became oligotrophic with traces only of some recycled nutrients

327 remaining at depth (Table 1).

328 Typically, this part of the Mediterranean is phosphorous limited [Pujo-Pay *et al.*,  
329 2006]. Commensurate with previous findings [Frayssé *et al.*, 2013], the upwelling seemed to  
330 decrease the dissolved NO<sub>3</sub>:PO<sub>4</sub> ratio, thereby turning the typical phosphorous into a  
331 upwelling-induced nitrogen limitation (Figure 4k, 5e and f). The near-shore surface NO<sub>3</sub>:PO<sub>4</sub>  
332 ratio on 13 October, i.e. immediately after the upwelling and prior to the intrusion was 2:1  
333 (Figure 5e-h), indicating a severe nitrogen limitation. Once the oligotrophic water from the  
334 Northern Current started to move onshore, the previously upwelled waters were replaced and  
335 the model showed a marked shift from N- back to P-limitation in phytoplankton  
336 photosynthesis (with NO<sub>3</sub>:PO<sub>4</sub> ratios reaching 40:1 in the surface waters, Figure 4l through  
337 o, Figure 5 e-h). The intrusion thus rendered the entire eastern Gulf phosphorous limited with  
338 Chl-*a* concentrations near the OC5 algorithm's detection limit and PO<sub>4</sub> concentrations in the  
339 surface layer dropping to below 0.01 mmol L<sup>-1</sup> (Figure 5g-h). As there are no *in situ* nutrient  
340 data to cover the entire temporal succession from pre-upwelling, over upwelling to intrusion,  
341 these last results should be regarded as preliminary only until they can be either verified or  
342 disproven by *in situ* observations. This would require a dedicated field campaign with daily  
343 measurements possibly lasting 10-14 days to monitor the entire series of events.

344 In a study in the north-western Gulf of Mexico, Chen *et al.* [2000] also observed a  
345 drop in primary production between 2 successive years which they attributed to the intrusion  
346 of oligotrophic offshore water. The difference in Chl concentration was less dramatic,  
347 however, and given the one year time difference between observations, results are not easily  
348 comparable.

349 In the Yangtze River Delta, Jiao *et al.* [2007] also observed an intrusion of warmer  
350 offshore water from the Kuroshio current, replacing Yangtze plume water and leading to a  
351 change in phytoplankton abundance. In contrast to the NC, the Kuroshio is a nutrient-rich

352 subsurface current. Its intrusion on the shelf near the Yangtze delta thus led to an increase in  
353 primary production, mainly due to the higher visibility and thus better light penetration in the  
354 Kuroshio water compared to the more turbid Yangtze plume water.

355 Studies that examined the intrusion of the oligotrophic subtropical extension of the  
356 East-Australian current onto the NW New Zealand shelf found a similar impact for the on-  
357 shelf primary production [Sharples, 1997; Zeldis, 2004; Zeldis *et al.*, 2004]. Due to the  
358 nitrogen limitation in the intruding waters, chlorophyll concentrations had dropped  
359 dramatically in the surface layer. However, in that particular case, the intrusion was limited to  
360 a shallow surface layer, which allowed phytoplankton to bloom at depth, i.e., at the interface  
361 between the clear surface waters and the nutrient rich bottom layer. Another striking effect  
362 that was caused by that intrusion was the introduction of offshore fish species and toxic  
363 phytoplankton species onto the shelf.

364 All these studies compared the effect of intrusions based on observations that were  
365 sometimes as far apart as 1 year [Chen *et al.*, 2000]. In contrast, the present work examined –  
366 for the first time to our knowledge - the actual dynamics of such intrusion events and could  
367 demonstrate how abrupt and significant these changes can be. Unfortunately, research on NC  
368 intrusions in the GoL is a rather recent field of research and much is still to be discovered  
369 about the response of and the possible impact on the wider ecosystem and higher trophic  
370 levels, including fisheries. From a management perspective, it would be important to know  
371 how these intrusions affect secondary producers. Changes in the discharge volume of the  
372 Rhone River into the GoL have been found to directly impact on the amount of landings of  
373 Common Sole (*Solea solea*) 5 years later (M. Harmelin, pers. comm.). It would seem like a  
374 plausible assumption that any possible impact due to changes in the frequency and/or  
375 magnitude of intrusions would also take about 5 years to penetrate to the upper levels of the  
376 food web. This is particularly relevant, considering that the GOL is the most productive and  
377 profitable region for fisheries in the Western Mediterranean and about 50% of the catch in the

378 GOL originates from areas which are directly affected by NC intrusions such as the one  
379 described in this study. However, no long term data on intrusions is available. It is only  
380 recently, that people have begun to look at the frequency and magnitude of NC intrusions.  
381 Findings, in particular by *Gatti et al. [Intrusions of the Mediterranean Northern Current on*  
382 *the eastern side of the Gulf of Lion's continental shelf: characterization and generating*  
383 *processes, submitted to Journal of Geophysical Research 2014]* and *Barrier et al. [2015]*,  
384 suggest that these intrusions are not only frequent but also rather large in terms of horizontal  
385 fluxes, and thus capable of inducing frequent and significant changes to the GOL ecosystem.  
386 Further observations and modelling efforts are urgently needed in order to fully describe  
387 these processes and their impact on the ecosystem in more detail.

388

## 389 **5. Acknowledgements**

390 The authors wish to acknowledge the Compagnie Nationale du Rhone for the Rhone  
391 River discharge data, as well as Meteo France for meteorological data. The mooring and  
392 satellite SST data were collected and made freely available by the MyOcean project and the  
393 programs that contribute to it. The authors thank the GFSC, Greenbelt, MD 20771, for the  
394 production and distribution of MODIS ocean color data, processed by IFREMER. The Rhone  
395 concentration data were provided by the National MOOSE Program and the Service  
396 d'Observation of the Mediterranean Institute of Oceanography (MIO), and the vessel  
397 mounted ADCP data by the technical staff of INSU in the framework of the SAVED  
398 platform. We also acknowledge B. Queguiner and D. Malengros for allowing the ADCP  
399 transects during the SPECIMED cruises, and all the technical staff involved in the  
400 RHOMA2011 IFREMER cruise. The authors acknowledge the staff of the "Cluster de calcul  
401 intensif HPC" Platform of the OSU Institut Pythéas (Aix-Marseille University, INSU-CNRS)  
402 for providing the computing facilities as well as M. Libes and C. Yohia for technical

403 assistance. This work was supported by an IFREMER/PACA regional grant, the GIRAC  
404 (AERMC) and MASSILIA (PNEC-EC2CO) projects. Additional support came from the  
405 MERMEX (WP3-C3A-Mistrals), IMBER and LOICZ as well as the European PERSEUS  
406 projects (EC grant agreement 287600). ONR wishes to acknowledge financial support from  
407 the People Programme (Marie Curie Actions) of the European Union's Seventh Framework  
408 Programme FP7/2007-2013/ under REA grant agreement n° 624170 as well as the AMICO-  
409 BIO project (12-MCGOT-GMES-1-CVS-047/MEDDE/CNRS-INSU). We also thank A.  
410 Petrenko, F. Diaz, M. Harmelin, and two anonymous reviewers for their helpful comments on  
411 the manuscript.

412

## 413 6. References

- 414 Alberola, C., and C. Millot (2003), Circulation in the French mediterranean coastal zone near  
415 Marseilles: the influence of wind and the Northern Current, *Continental Shelf*  
416 *Research*, 23(6), 587-610.
- 417 Alberola, C., C. Millot, and J. Font (1995), On the Seasonal and Mesoscale Variabilities of  
418 the Northern Current during the Primo-O Experiment in the Western Mediterranean-  
419 Sea, *Oceanologica Acta*, 18(2), 163-192.
- 420 Andre, G., P. Garreau, and P. Fraunie (2009), Mesoscale slope current variability in the Gulf  
421 of Lions. Interpretation of in-situ measurements using a three-dimensional model,  
422 *Continental Shelf Research*, 29(2), 407-423.
- 423 Antoine, D., F. d'Ortenzio, S. B. Hooker, G. Becu, B. Gentili, D. Tailliez, and A. J. Scott  
424 (2008), Assessment of uncertainty in the ocean reflectance determined by three  
425 satellite ocean color sensors (MERIS, SeaWiFS and MODIS-A) at an offshore site in  
426 the Mediterranean Sea (BOUSSOLE project), *J Geophys Res-Oceans*, 113(C7).
- 427 Baklouti, M., V. Faure, L. Pawlowski, and A. Sciandra (2006a), Investigation and sensitivity  
428 analysis of a mechanistic phytoplankton model implemented in a new modular  
429 numerical tool (Eco3M) dedicated to biogeochemical modelling, *Progress In*  
430 *Oceanography*, 71(1), 34-58.
- 431 Baklouti, M., F. Diaz, C. Pinazo, V. Faure, and B. Queguiner (2006b), Investigation of  
432 mechanistic formulations depicting phytoplankton dynamics for models of marine  
433 pelagic ecosystems and description of a new model, *Progress In Oceanography*,  
434 71(1), 1-33.
- 435 Barrier, N., A. A. Petrenko, and Y. Ourmières (2015), Strong intrusions of the Northern  
436 Mediterranean Current on the eastern Gulf of Lion: insights from in-situ observations  
437 and high resolution numerical modelling, *Ocean Dynamics*, accepted.

- 438 Chen, X., S. E. Lohrenz, and D. A. Wiesenburg (2000), Distribution and controlling  
439 mechanisms of primary production on the Louisiana–Texas continental shelf, *Journal*  
440 *of Marine Systems*, 25(2), 179-207.
- 441 Coste, B. (1974), Role des apports nutritifs minéraux rhodaniens sur la production organique  
442 des eaux du Golfe du Lion, *Tethys*, 6, 727-740.
- 443 de Madron, X. D., et al. (2011), Marine ecosystems' responses to climatic and anthropogenic  
444 forcings in the Mediterranean (vol 91, pg 97, 2011), *Progress in Oceanography*,  
445 91(4), 593-594.
- 446 Echevin, V., M. Crepon, and L. Mortier (2003), Interaction of a coastal current with a gulf:  
447 Application to the shelf circulation of the Gulf of Lions in the Mediterranean Sea,  
448 *Journal of Physical Oceanography*, 33(1), 188-206.
- 449 El Sayed, M. A., A. Aminot, and R. Kerouel (1994), Nutrients and Trace-Metals in the  
450 Northwestern Mediterranean under Coastal Upwelling Conditions, *Continental Shelf*  
451 *Research*, 14(5), 507-530.
- 452 Estournel, C., X. D. de Madron, P. Marsaleix, F. Auclair, C. Julliand, and R. Vehil (2003),  
453 Observation and modeling of the winter coastal oceanic circulation in the Gulf of Lion  
454 under wind conditions influenced by the continental orography (FETCH experiment),  
455 *J Geophys Res-Oceans*, 108(C3).
- 456 Faure, V., C. Pinazo, J. P. Torreton, and P. Douillet (2010a), Modelling the spatial and  
457 temporal variability of the SW lagoon of New Caledonia II: Realistic 3D simulations  
458 compared with in situ data, *Mar Pollut Bull*, 61(7-12), 480-502.
- 459 Faure, V., C. Pinazo, J. P. Torreton, and S. Jacquet (2010b), Modelling the spatial and  
460 temporal variability of the SW lagoon of New Caledonia I: A new biogeochemical  
461 model based on microbial loop recycling, *Mar Pollut Bull*, 61(7-12), 465-479.
- 462 Fraysse, M. (2014), Rôle du forçage physique sur l'écosystème à l'est du Golfe du Lion:  
463 modulation de l'impact des apports anthropiques en sels nutritifs et matière organique  
464 étudiée par modélisation 3D couplée physique et biogéochimique, PhD thesis, 338 pp,  
465 Aix-Marseille University, Marseille, France.
- 466 Fraysse, M., I. Pairaud, O. N. Ross, V. M. Faure, and C. Pinazo (2014), Intrusion of Rhone  
467 River diluted water into the Bay of Marseille: Generation processes and impacts on  
468 ecosystem functioning, *J Geophys Res-Oceans*, 119.
- 469 Fraysse, M., C. Pinazo, V. M. Faure, R. Fuchs, P. Lazzari, P. Raimbault, and I. Pairaud  
470 (2013), Development of a 3D Coupled Physical-Biogeochemical Model for the  
471 Marseille Coastal Area (NW Mediterranean Sea): What Complexity Is Required in the  
472 Coastal Zone?, *PLOS ONE*, 8(12).
- 473 Gatti, J., A. Petrenko, J.-L. Devenon, Y. Leredde, and C. Ulses (2006), The Rhone river  
474 dilution zone present in the northeastern shelf of the Gulf of Lion in December 2003,  
475 *Continental Shelf Research*, 26(15), 1794-1805.
- 476 Gohin, F., S. Loyer, M. Lunven, C. Labry, J. M. Froidefond, D. Delmas, M. Huret, and A.  
477 Herbland (2005), Satellite-derived parameters for biological modelling in coastal  
478 waters: Illustration over the eastern continental shelf of the Bay of Biscay, *Remote*  
479 *Sensing of Environment*, 95(1), 29-46.
- 480 Jiao, N., et al. (2007), Ecological anomalies in the East China Sea: Impacts of the Three  
481 Gorges Dam?, *Water Research*, 41(6), 1287-1293.

- 482 Lazure, P., and F. Dumas (2008), An external-internal mode coupling for a 3D  
483 hydrodynamical model for applications at regional scale (MARS), *Adv Water Resour*,  
484 *31*(2), 233-250.
- 485 Millot, C. (1990), The Gulf of Lions Hydrodynamics, *Continental Shelf Research*, *10*(9-11),  
486 885-894.
- 487 Millot, C. (1999), Circulation in the Western Mediterranean Sea, *Journal of Marine Systems*,  
488 *20*(1-4), 423-442.
- 489 Millot, C., and L. Wald (1980), The Effect of Mistral Wind on the Ligurian Current near  
490 Provence, *Oceanologica Acta*, *3*(4), 399-402.
- 491 Morel, A., A. Bricaud, J. M. Andre, and J. Pelaez-Hudlet (1990), Spatial- temporal evolution  
492 of the Rhone plume as seen by CZCS imagery. Consequences upon the primary  
493 production in the Gulf of Lion., in *Water Pollution Research Reports of the European*  
494 *Communities*, edited by J. M. Martin and H. Barth, pp. 45-62, NERC, Plymouth, UK.
- 495 Pairaud, I. L., J. Gatti, N. Bensoussan, R. Verney, and P. Garreau (2011), Hydrology and  
496 circulation in a coastal area off Marseille: Validation of a nested 3D model with  
497 observations, *Journal of Marine Systems*, *88*(1), 20-33.
- 498 Petrenko, A. (2003), Variability of circulation features in the gulf of lion NW Mediterranean  
499 Sea. Importance of inertial currents, *Oceanologica Acta*, *26*(4), 323-338.
- 500 Petrenko, A., Y. Leredde, and P. Marsaleix (2005), Circulation in a stratified and wind-forced  
501 Gulf of Lions, NW Mediterranean Sea: in situ and modeling data, *Continental Shelf*  
502 *Research*, *25*(1), 7-27.
- 503 Petrenko, A., C. Dufau, and C. Estournel (2008), Barotropic eastward currents in the western  
504 Gulf of Lion, north-western Mediterranean Sea, during stratified conditions, *Journal*  
505 *of Marine Systems*, *74*(1-2), 406-428.
- 506 Petrenko, A., M. Kersale, F. Nencioli, J. Gatti, and I. Dekeyser (2013), Coastal circulation in  
507 the Gulf of Lion, the influence of mesoscale processes on interregional exchanges,  
508 paper presented at 40th CIESM Congress, Marseille, France.
- 509 Pinazo, C., P. Marsaleix, B. Millet, C. Estournel, and R. Vehil (1996), Spatial and temporal  
510 variability of phytoplankton biomass in upwelling areas of the northwestern  
511 Mediterranean: A coupled physical and biogeochemical modelling approach, *Journal*  
512 *of Marine Systems*, *7*(2-4), 161-191.
- 513 Pujo-Pay, M., P. Conan, F. Joux, L. Oriol, J. J. Naudin, and G. Cauwet (2006), Impact of  
514 phytoplankton and bacterial production on nutrient and DOM uptake in the Rhone  
515 river plume (NW Mediterranean), *Marine Ecology Progress Series*, *315*, 43-54.
- 516 Rubio, A., V. Taillandier, and P. Garreau (2009), Reconstruction of the Mediterranean  
517 northern current variability and associated cross-shelf transport in the Gulf of Lions  
518 from satellite-tracked drifters and model outputs, *Journal of Marine Systems*, *78*, S63-  
519 S78.
- 520 Schaeffer, A., A. Molcard, P. Forget, P. Fraunié, and P. Garreau (2011), Generation  
521 mechanisms for mesoscale eddies in the Gulf of Lions: radar observation and  
522 modeling, *Ocean Dynamics*, *61*, 1587-1609.
- 523 Sempere, R., B. Charriere, F. Van Wambeke, and G. Cauwet (2000), Carbon inputs of the  
524 Rhone River to the Mediterranean Sea: Biogeochemical implications, *Global*  
525 *Biogeochemical Cycles*, *14*(2), 669-681.

- 526 Sharples, J. (1997), Cross-shelf intrusion of subtropical water into the coastal zone of  
527 northeast New Zealand, *Continental Shelf Research*, 17(7), 835-857.
- 528 Volpe, G., S. Colella, V. Forneris, C. Tronconi, and R. Santoleri (2012), The Mediterranean  
529 Ocean Colour Observing System - system development and product validation, *Ocean*  
530 *Science*, 8(5), 869-883.
- 531 Zeldis, J. R. (2004), New and remineralised nutrient supply and ecosystem metabolism on the  
532 northeastern New Zealand continental shelf, *Continental Shelf Research*, 24(4-5),  
533 563-581.
- 534 Zeldis, J. R., R. A. Walters, M. J. N. Greig, and K. Image (2004), Circulation over the  
535 northeastern New Zealand continental slope, shelf and adjacent Hauraki Gulf, during  
536 spring and summer, *Continental Shelf Research*, 24(4-5), 543-561.
- 537